Artificially Intelligent Power Amplifier Array (AIPAA): A New Paradigm in Reconfigurable Radar Transmission

Charles Baylis
Department of Electrical and Computer Engineering
Baylor University
Waco, USA
Charles_Baylis@baylor.edu

Robert J. Marks II
Department of Electrical and Computer Engineering
Baylor University
Waco, USA
Robert_Marks@baylor.edu

Austin Egbert
Department of Electrical and Computer Engineering
Baylor University
Waco, USA
Austin_Egbert@baylor.edu

Casey Latham
Keysight Technologies
Austin, USA
casey.latham@keysight.com

Abstract – The increasing re-allocation of traditional radar bands for spectrum sharing requires future radar systems to be both adaptive and reconfigurable in real time. Radar array outputs must be monitored so that related inputs are adjusted to ensure spatial and spectral coexistence with other systems while maximizing performance. We discuss a new concept: an array of reconfigurable power amplifiers coupled with fast algorithms that can allow performance to be re-optimized upon changes in operating frequency or beam steering. This AIPAA will be capable of embedding artificial intelligence (AI) and machine learning (ML) techniques to optimize the array pattern with the waveforms and circuitry. The AIPAA will optimize the transmitter and transmissions to coexist within the spectral and spatial domains. A spatial-spectral mask and an approach to join different optimizations are discussed as useful building blocks for constructing the AIPAA optimizations. The impact of circuit linearity on the array pattern and potential improvement from real-time reconfigurable circuitry in the array elements are also discussed.

Keywords – cognitive radar, power amplifiers, radio spectrum management, spectrum sharing.

I. INTRODUCTION

The congested wireless spectrum and its continued re-allocation require future radar systems to be both adaptive and reconfigurable. To date, 3.45 GHz to 3.7 GHz from the United States S-band radar allocation has been re-allocated for sharing between radar and wireless communications, with a recent ruling allocating the 3.45 GHz to 3.55 GHz to fifth-generation (5G) wireless communications as the primary user [1]. The 3.55 GHz to 3.7 GHz band has been allocated for sharing between radar, the Citizens Band Radio Service (CBRS) [2], and the 4G and 5G wireless transmissions [2]. Additionally, the 3.1 to 3.45 GHz subband has also been proposed for sharing [3]. The use of a phased array enables the radar transmitter to perform directional and potentially multiple-beam transmissions to increase spectrum efficiency. Transmitter arrays must be able to reconfigure quickly, changing direction and beam pattern to coexist with communications in this band.

Recent development of high-power reconfigurable circuit technology suitable for radar use [4] has made possible the concept of reconfigurable transmitter amplifiers. Using reconfigurable power amplifiers as building blocks within the array elements, real-time optimizations of array power-amplifier circuitry, phase shifts, and excitation waveforms are needed to maximize the sharing of finite spectral and spatial resources. AI and ML are expected to be useful in successfully and efficiently combining these multi-parameter, multi-objective optimizations. While typical prior applications of AI in radar have been limited to target tracking and recognition, control and enhanced performance, and signal processing and synthesis; the further application of AI and ML to optimizing transmission waveforms, circuits, and arrays in an AIPAA will allow performance to be optimized when changing operating frequency or scan angle in a spectrum sharing environment.

II. AIPAA

A block diagram of the AIPAA is shown in Fig. 1. The AIPAA must perform a multi-objective optimization to achieve the goals of range, power efficiency, and spectral and spatial containment.
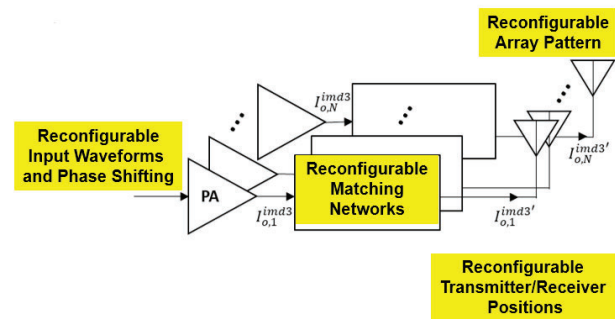
Fig. 1. AIPAA Block Diagram

The AIPAA will contain the ability to re-match its power amplifiers "on the fly" with reconfigurable matching networks. This will allow power to be optimized on transmission, which maximizes the range of the transmission, while also maximizing the power-added efficiency (PAE) and meeting spectral and spatial constraints. Single-element circuit optimization techniques must be expanded to allow multi-amplifier optimizations in the array. Qiao demonstrates adaptive power-amplifier matching in traditional microwave-band transmissions [5]. Semnani has demonstrated a 90-W RF power handling impedance tuner designed for radar transmissions in the S-band from 3.1 to 3.5 GHz [4].

In the AIPAA, the input waveforms and phase shifting should be adjusted in concert with the impedance tuners in each element to meet the aforementioned multiple objectives. Eventually, each "element" may move physically throughout a

specified geographic area, potentially changing the array configuration.

II. REAL-TIME IMPEDANCE TUNING

The use of amplifier load-impedance reconfiguration for use in arrays has been explored by Rodriguez-Garcia for single- and dual-beam array transmission [6, 7]. The tuning of an amplifier's load impedance can affect the range and the spectral mask compliance of the transmission. A single-element experiment by Alcala-Medel [8] shows a three-frequency reconfiguration measurement experiment from which the calculated range (based on measured output power) and measured spectral mask compliance were plotted against measurement number, as shown in Fig. 2. Since a radar application was envisioned in this reference, the radar range was calculated from the measured output power using assumed radar system parameters. The spectral mask metric S_m is defined such that mask compliance is obtained for $S_m \leq 0$ [9]. Fig. 2 shows that the range is reduced upon changing frequency without re-tuning (visible at measurements 12 and 25). At measurement 12 where the system changes from 3.3 GHz to 3.1 GHz, the S_m value goes up from 0 to almost 2, transitioning from compliance to significant non-compliance. Re-tuning allows both the range and spectral mask compliance to be improved/restored after shifting to 3.1 GHz. Similar effects occur upon the shift to 3.5 GHz, followed by improvements resulting from impedance tuning. While Rodriguez-Garcia has shown that impedance tuning can reduce spurious emissions in arrays while maximizing element gain [7], such optimizations (to be performed in real time) will require global monitoring of the entire array and optimization of the entire system. Intelligent measurement, monitoring, optimization, and control techniques will be crucial. Techniques such as the *in situ* impedance sensor designed by Donahue [10] will be useful in assessing system performance during optimization.
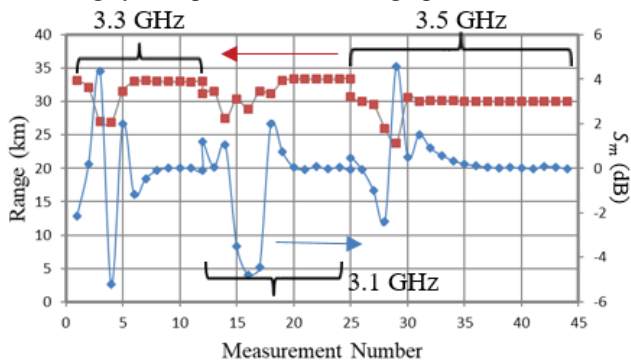
Fig. 2. Range and spectral mask compliance metric S_m versus measurement number. Reprinted from [9].

II. SPATIAL-SPECTRAL MASK FOR COEXISTENCE

Because many radars use phased arrays, they have the capability to promote coexistence through directional transmission. We have suggested the use of a spatial-spectral mask for coexistence in directional transmissions, as introduced by Egbert [11]. If the maximum interference power received by each receiver in the geographic vicinity of a transmitter is made available, then the needed spatial-spectral mask to preserve coexistence can be calculated using the Friis transmission equation. Fig. 3 shows an example of the spatial-spectral mask. The spatial-spectral mask can be used as a constraint in an optimization routine that maximizes quality of service [11].

If the maximum interference spatial-spectral power density tolerable by each device $P_r(f, R, \phi)$ is known based on its frequency f, and its radius R and angle $\emptyset$ from the transmitter, then the power that can be transmitted per Hz bandwidth and per radian angle is shown in [11] to be given, based on the Friis equation, by

$$P_t(f, \phi) = \min_{0 \leq R \leq \infty} \left[P_r(f, R, \phi) \frac{(4\pi R)^2}{2\pi G_r \lambda^2} \right], \qquad (1)$$

Egbert also shows that, given a transmission pattern $G_t(\phi)$, a spectral power density constraint map can be derived, given by [11] as:

$$S_t(f) = \int_0^{2\pi} \min_{0 \leq \phi \leq 2\pi} \left[P_t(f, \phi) \frac{1}{G_t(\phi)} \right] d\phi. \qquad (2)$$

Similarly, for a given a normalized transmission spectrum $X(f)$, a spatial power density constraint map can be derived, also shown in [11]:

$$Q_t(\phi) = \int_{f_1}^{f_2} \min_{f_1 \leq f \leq f_2} \left[P_t(f, \phi) \frac{1}{|X(f)|} \right] df, \qquad (3)$$
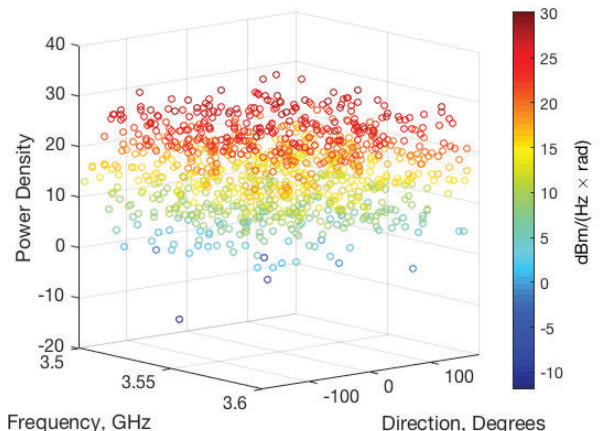
Fig. 3. Maximum transmission power density at different frequency-direction combinations (based on relative transmitter and receiver locations and connectable into a spatial-spectral mask). Reprinted from [11].

Given the spectral mask requirements that can be generated based on a known transmission pattern, waveform optimization can be used to obtain a desired ambiguity function, while meeting the spectral mask constraints derived from the spectral/spatial mask constraints. An example was given by Egbert [11] that shows the development of a range-oriented radar for an ideal beam steered to a center angle of 60° with a beam width of 30°, over which the transmission is isotropic. Fig. 4 shows the ambiguity function template, which minimizes the ambiguity away from the Doppler axis (Fig. 4(a)), along with the ambiguity function of the achieved waveform (Fig. 4(b)). The spectrum of the optimized waveform is shown with the spectral mask in Fig. 4(c) [11]. As expected for a range-oriented radar, the waveform optimization results in a

waveform with wide bandwidth that meets the spectral mask constraints.

A similar situation is expected to exist for the application of the spatial mask, using a given waveform. The array will be optimized to obtain desired beamforming characteristics, but will be subjected to the spatial mask constraints created based on the frequency content of the waveform.

In the AIPAA system, joint optimization of the waveform, array, and circuit is desired to maximize all objectives simultaneously. The concept of merging optimizations must be addressed in detail in the future. First efforts toward optimization merging are explained in the next section.
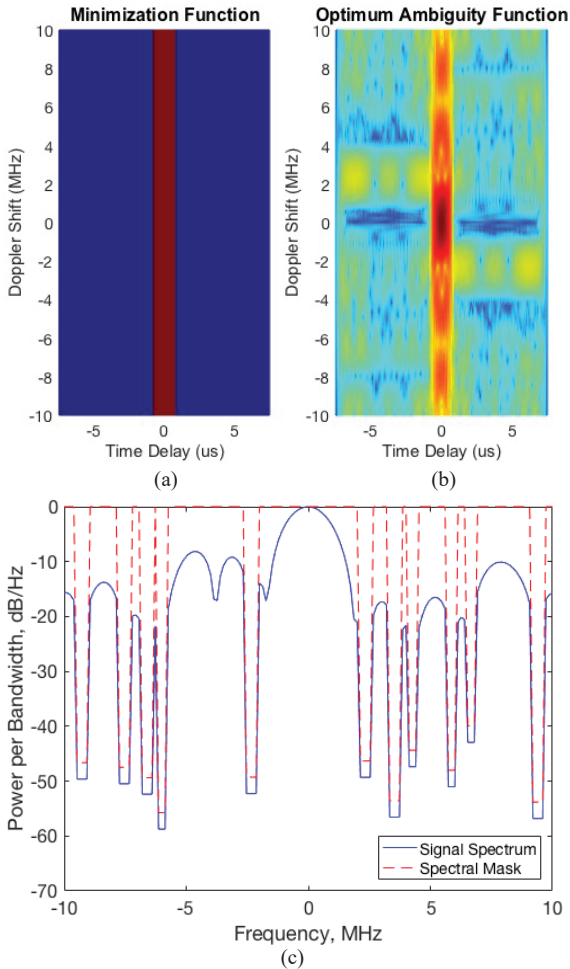
Fig. 4. (a) Ambiguity function minimization template, with the minimization region shown in blue, (b) ambiguity function of the optimized waveform, and (c) power spectral density of the optimized waveform, shown with the spectral mask. Reprinted from [11].

III. JOINT OPTIMIZATIONS

Merging the optimizations of the circuit, array, and waveform to achieve a defined multi-objective success is a key challenge of the AIPAA. A reasonable first step toward this challenge is to combine optimizations of the different parameters in small steps. As an example of combining two disparate optimizations, we present the joining of optimizations of a radar transmitter circuit with that of the waveform, as

presented by Latham [12]. A gradient-based circuit optimization was interwoven with an ambiguity-function based waveform optimization. Each waveform optimization iteration was assumed to require only one-fifth of the time of an impedance tuning iteration. To depict this scenario, a sequence of five waveform optimization steps, followed by one circuit optimization step, was performed. The overall optimization seeks to match the radar range/Doppler ambiguity function to a template while maximizing the PAE and meeting spectral mask constraints. Fig. 5 shows a block diagram of the joint circuit and waveform optimization procedure.
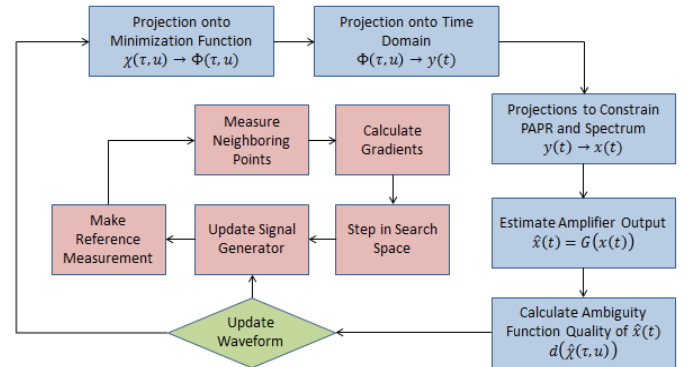
Fig. 5. Joint circuit and waveform optimization procedure, reprinted from [12].

Fig. 6 shows a comparison of the joint (one circuit iteration followed by five waveform iterations) and sequential (complete circuit optimization followed by complete waveform optimization) optimizations [12]. The sequential optimization (Fig. 6(a)) (which completely optimizes the circuit first) results in a quick rise in PAE. However in Fig. 6(b), a corresponding very large least-squares distance from the ambiguity-function template results for the first half of the sequential search, indicating poor range/Doppler ambiguity function performance of the transmitted waveform. The joint optimization provides gradual raising of PAE to its final value, and a much better (lower) least-squares distance through the entire search, indicating a radar waveform with more desirable resolution. Fig. 6(c) shows that the spectral mask limitations are also reached more quickly in the joint optimization, because the desired high-bandwidth waveform appears earlier in the search. Joint optimization allows a compromise of all objectives to be reached in a quicker manner.

To illustrate the benefit of using joint optimization to ensure all objectives are optimized quickly, Fig. 7 shows the ambiguity function of the measured waveforms for the joint and sequential optimizations at equivalent waveform iteration 26 (an iteration of the circuit optimization accounts for 5 equivalent waveform iterations) [12]. The ambiguity function from the joint optimization shows good agreement with the template, while the ambiguity function from the sequential optimization (the circuit is optimized first) does not show good agreement with the template. This corresponds with the large disparity in least-squares distance between the joint circuit and waveform optimizations visible in Fig. 6(b) for a value of 26 on the horizontal axis.

(a)

(b)

(c)
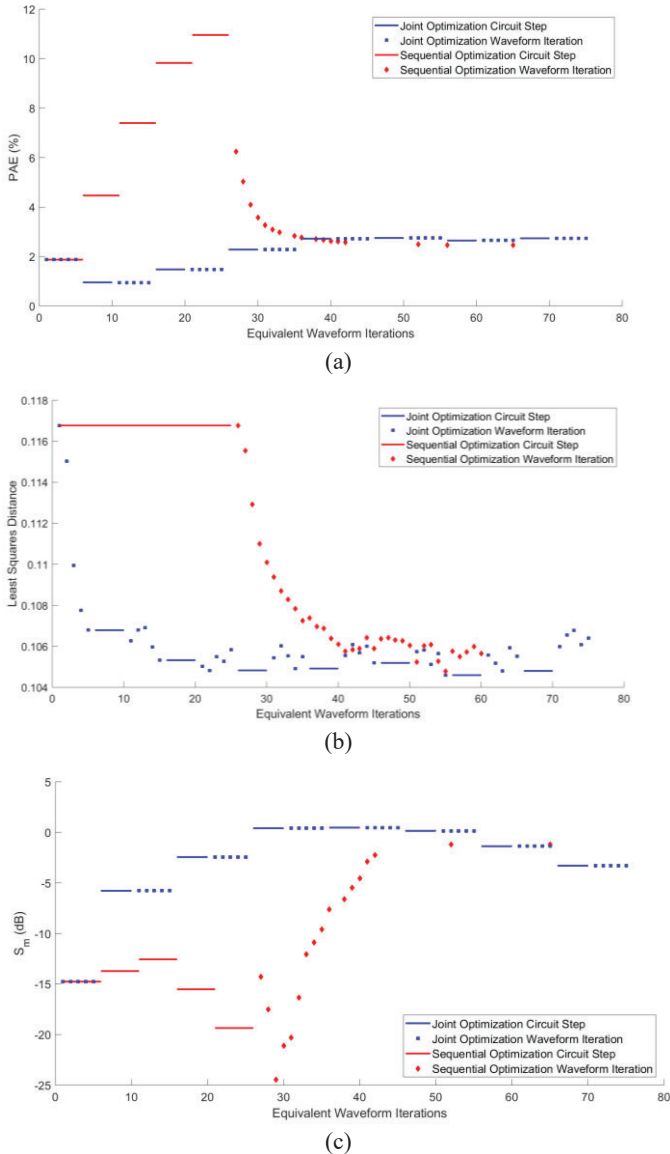
Fig. 6. Comparisons of (a) PAE, (b) least-squares distance between the range/Doppler ambiguity function and its template, and (c) spectral mask compliance metric S_m. Reprinted from [12].

The AIPAA requires joint optimizations of the circuit, waveform, array excitations (including phase shifts) and possibly the array element positions. As the numbers of objectives and parameters are increased, AI and ML are expected to increase their roles in making joint optimizations efficient. These searches will likely be framed as multi-objective and constrained optimizations, and domain expertise should be used to enhance learning algorithms for application to the AIPAA. While AI and ML can be useful if they fit the context to which they are applied, blindly using AI to try to sort out optimization problems is a dangerous pitfall. Trendy AI techniques, such as Deep Convolutional Neural Networks, and Reinforcement Learning, while potentially useful in certain scenarios, have significant limitations. Such techniques should be used only in applications for which they are designed.
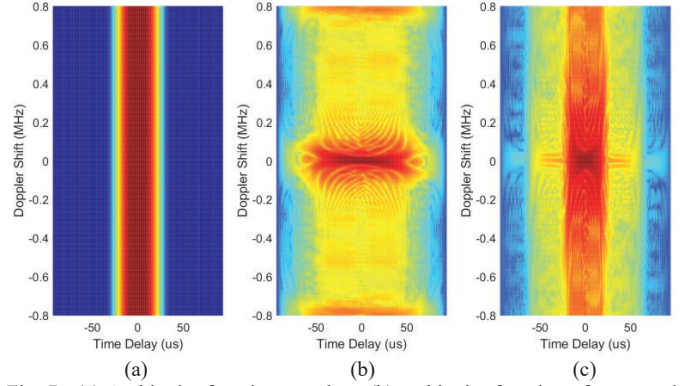
Fig. 7. (a) Ambiguity function template, (b) ambiguity function of measured waveform at equivalent waveform iteration 26 for the sequential optimization, and (c) ambiguity function of measured waveform at equivalent waveform iteration 26 for the joint optimization. Reprinted from [12].

IV. EFFECT OF IMPEDANCE TUNING ON ARRAY PATTERN

The effects of impedance tuning on array patterns are less widely documented in the literature than the effects of impedance tuning on the spectrum. However, since the linearity of the transmitter power amplifier depends significantly on its load impedance, the load impedance influences the array pattern fidelity through the linearity (or nonlinearity) of the power amplifier. As two-tone spectra can be used to show the generation of nonlinear intermodulation products through the nonlinear amplifier's creation of two (or more) additional tones, the input of two beam kernels to a power amplifier results in the creation of two (or more) additional unwanted beams to be generated [13, 14]. In general, a combined spectral-spatial intermodulation can occur from a dual-beam, dual-tone transmission, as shown by Hemmi [15] and Haupt [16].

Since it has been shown that nonlinearities in the power amplifier can cause unwanted beam effects; it stands to reason that impedance tuning, which can be used to linearize the power amplifier, can be used to provide a cleaner beam pattern in the same manner used to provide a clean transmission spectrum. Rodriguez-Garcia demonstrates the use of impedance tuning to maximize power-amplifier gains in the individual elements of an array, while increasing the beam pattern fidelity, both in single-beam [6] and dual-beam [7] cases.

Moving forward, these optimizations should be integrated with real-time evaluation measurements. Real-time array optimization algorithms must be created that allow efficient optimization of impedance tuners in the array elements. These optimizations will rely on real-time *in situ* measurements that are capable of measuring critical elements to determine the spatial distortion and the gain values of the individual amplifiers. The development of *in situ* measurement techniques, such as an impedance sensor recently demonstrated by Donahue [10], that can be used in the array elements is a high priority in developing this technology.

Given the benefits of impedance tuning in cleaning transmissions in both the spectral and spatial domain, the combined optimization approach joining circuit and waveform optimization of Latham [12] must be extended to envelop the

spatial domain as well. The growing complexity of this optimization problem suggests that AI and ML, utilizing domain expertise, may be useful tools if appropriately applied.

V. Conclusions

The AIPAA will merge array, circuit, and waveform optimizations for successfully sharing spectrum resources with users in directional transmissions, such as 5G Long Term Evolution mmW communications and array radar systems. Use of a joint spectral and spatial mask in constraining optimizations and an approach for joining optimizations have been described as useful techniques for constraining and merging optimizations in the AIPAA.

References

[1] "Fact Sheet: Facilitating 5G in the 3.45-3.55 GHz Band, Report and Order and Further Notice of Proposed Rulemaking: WT-Docket No. 19-348," Federal Communications Commission, September 2020, https:///docs.fcc.gov/public/attachments/DOC-366780A1.pdf.

[2] Federal Communications Commission Rulemaking 12-354: "3.5 GHz Band / Citizens Broadband Radio Service," https://www.fcc.gov/wireless/bureau-divisions/broadband-division/35-ghz-band/35-ghz-band-citizens-broadband-radio.

[3] Federal Communications Commission, "FCC Considers Facilitating Shared Use in the 3.1-3.55 GHz Band," DA/FCC# FCC-19-130, https://www.fcc.gov/document/fcc-considers-facilitating-shared-use-31-355-ghz-band-0.

[4] A. Semnani, G.S. Shaffer, M.D. Sinanis, and D. Peroulis, "High-Power Impedance Tuner Utlising Substrate-Integrated Evanescent-Mode Cavity Technology and External Linear Actuators," *IET Microwaves, Antennas & Propagation*, Vol. 13, No. 12, October 2019, pp. 2067-2072.

[5] D. Qiao, R. Molfino, S.M. Lardizabal, B. Pillans, P. Asbeck, and G. Jerinic, "An Intelligently Controlled RF Power Amplifier With a Reconfigrable MEMS-Varactor Tuner," *IEEE Transactions on Microwave Theory and Techniques*, Vol. 53, No. 3, Part 2, March 2005, pp. 1089-1095.

[6] P. Rodriguez-Garcia, J. Sifri, C. Calabrese, C. Baylis, and R.J. Marks II, "Range Improvement in Single-Beam Phased Array Radars by Amplifier Impedance Tuning," submitted to *IEEE Transactions on Antennas and Propagation*, January 2020.

[7] P. Rodriguez-Garcia, J. Sifri, C. Calabrese, C. Baylis, and R.J. Marks II, "Spurious Beam Suppression in Dual-Beam Phased Array Transmission by Impedance Tuning," submitted to *IEEE Transactions on Aerospace and Electronic Systems*, August 2020.

[8] M. Fellows, J. Barlow, C. Baylis, J. Barkate, R.J. Marks II, "Designing Power Amplifiers for Spectral Compliance Using Spectral Mask Load-Pull Measurements," 2015 IEEE Conference on Power Amplifiers for Wireless and Radio Applications (PAWR), San Diego, California, January 2015.

[9] J. Alcala-Medel, A. Egbert, C. Calabrese, A. Dockendorf, C. Baylis, G. Shaffer, A. Semnani, D. Peroulis, A. Martone, E. Viveiros, and R.J. Marks II, "Fast Frequency-Agile Real-Time Optimization of High-Power Tuning Network for Cognitive Radar Applications," 2019 IEEE MTT-S International Microwave Symposium, Boston, Massachusetts, June 2019.

[10] D. Donahue and T. Barton, "A 2-GHz Sampled Line Impedance Sensor for Power Amplifier Applications with Varying Load Impedance," 2019 IEEE Topical Conference on RF/Microwave Power Amplifiers for Wireless and Radio Applications (PAWR)," Orlando, Florida, January 2019.

[11] A. Egbert, C. Latham, C. Baylis, and R.J. Marks II, "Multi-Dimensional Coexistence: Using a Spatial-Spectral Mask for Spectrum Sharing in Directional Radar and Communication," 2018 Texas Symposium on Wireless and Microwave Circuits and Systems, Waco, Texas, April 2018.

[12] C. Latham, A. Egbert, C. Baylis, L. Cohen, and R.J. Marks II, "Joint Radar Amplifier Circuit and Waveform Optimization for Ambiguity Function, Power-Added Efficiency, and Spectral Compliance," *IEEE Transactions on Aerospace and Electronic Systems*, Vol. 55, No. 3, June 20///19, pp. 1190-1199.

[13] W.A. Sandrin, "Spatial Distribution of Intermodulation Products in Active Phased Array Antennas," *IEEE Transactions on Antennas and Propagation*, Vol. 21, No. 6, November 1973, pp. 864-868.

[14] E.G. Larsson and L. Van Der Pierre, "Out-of-Band Radiation from Antenna Arrays Clarified," *IEEE Wireless Communications Letters*, Vol. 7, No. 4, August 2018, pp. 610-613.

[15] C. Hemmi, "Pattern Characteristics of Harmonic and Intermodulation Products in Broad-Band Active Transmit Arrays," *IEEE Transactions on Antennas and Propagation*, Vol. 50, No. 6, June 2002, pp. 858-865.

[16] R.L. Haupt, "Antenna Arrays in the Time Domain: An Introduction to Timed Arrays," *IEEE Antennas and Propagation Magazine,* Vol. 59, No. 3, June 2017, pp. 33-41.